

## Size effect law and fracture mechanics of the triggering of dry snow slab avalanches

Zdeněk P. Bažant and Goangseup Zi

Department of Civil Engineering, Northwestern University, Evanston, Illinois, USA

David McClung

Department of Geography, University of British Columbia, Vancouver, British Columbia, Canada

Received 20 March 2002; revised 8 August 2002; accepted 18 November 2002; published 25 February 2003.

[1] A size effect law for fracture triggering in dry snow slabs of high enough length-to-thickness ratio is formulated, based on simplified one-dimensional analysis by equivalent linear elastic fracture mechanics. Viscoelastic effects during fracture are neglected. The derived law, which is analogous to Bažant's energetic size effect law developed for concrete and later for sea ice, fiber composites, rocks, and ceramics, is shown to agree with two-dimensional finite element analysis of mode II cohesive crack model with a finite residual shear stress. Fitting the proposed size effect law to fracture data for various slab thicknesses permits identifying the material fracture parameters. The value of preexisting shear stress in a thin weak zone of finite length is shown to have significant effect. There exists a certain critical snow depth, depending on the preexisting stress value, below which the size effect disappears. Practical applications require considering that the material properties (particularly the mode II fracture toughness or fracture energy) at the snow slab base are not constant but depend strongly on the slab thickness. This means that one must distinguish the material size effect from the structural size effect, and the combined size effect law must be obtained by introducing into the structural size effect law dependence of its parameters on snow thickness. The thickness dependence of these parameters can be obtained by matching the combined law to avalanche observations. Matching Perla's field data on 116 avalanches suggests that the mode II fracture toughness is approximately proportional to 1.8 power of snow thickness.

*INDEX TERMS:* 1827 Hydrology: Glaciology (1863); 1863 Hydrology: Snow and ice (1827); 3210 Mathematical Geophysics: Modeling; 3220 Mathematical Geophysics: Nonlinear dynamics; 8020 Structural Geology: Mechanics; *KEYWORDS:* snow, avalanches, scaling, size effect, fracture mechanics

**Citation:** Bažant, Z. P., G. Zi, and D. McClung, Size effect law and fracture mechanics of the triggering of dry snow slab avalanches, *J. Geophys. Res.*, 108(B2), 2119, doi:10.1029/2002JB001884, 2003.

### 1. Introduction

[2] There are two types of dry snow avalanches: (1) loose avalanches characterized by surface failures in snow that lacks cohesion and (2) slab avalanches characterized by snow which is cohesive enough to form a slab. Dry slab avalanches (the subject of this paper) are much larger and more destructive than loose snow avalanches [McClung and Schaerer, 1993; Daerr and Douady, 1999], and are responsible for most of the damage from avalanches.

[3] Dry snow slab avalanches initiate as brittle fractures in which the failure process becomes dynamic as soon as it is triggered. A drop of friction at the base after the layer of snow begins to slide is a common characteristic. As a result, the failure cannot be described in terms of plasticity, but fracture mechanics must be used. The sliding surface behaves as a shear (mode II) crack in which the initial

frictional stress,  $\tau_f$ , has been reduced to some small finite residual value,  $\tau_r$ .

[4] Slides in overconsolidated clay are a similar phenomenon. Their fracture character was postulated by Palmer and Rice [1973]. They considered the fracture process zone at the front of a sliding crack to have some nonnegligible finite length (denoted here as  $2c_f$ ) and formulated the failure condition in terms of Rice's J integral.

[5] In plasticity, the mechanical failure criterion is expressed in terms of the stress and strain tensors and their invariants. Such a criterion in general implies that there is no size effect, i.e., geometrically similar small and large structures fail at the same maximum stress, or at the same nominal stress  $\sigma_N$ , defined as the average stress in a cross section of the structure. In fracture mechanics, by contrast, the material failure criterion is expressed in terms of either the energy release rate or the stress-displacement relation of the opening crack. This is now known to automatically imply a size effect on the nominal strength of the structure.

[6] The necessity of a size effect on clay slides was recognized, and its form discussed, by *Palmer and Rice* [1973], although without attempting to obtain an approximate general formula. A size effect in dry slab avalanches has been inferred from observations of avalanche fracture lines [*Perla*, 1971; *McClung*, 1979]. The study of *Palmer and Rice* [1973] was applied to the dry slab avalanches to formulate the crack propagation criteria for a dry snow slab [*McClung*, 1979, 1981].

[7] This study is aimed at obtaining a simple general analytical formula of asymptotic matching type through the use of equivalent linear elastic fracture mechanics (LEFM) and verifying it numerically by a two-dimensional cohesive crack model. The asymptotic analysis is based on a simplified model of one-dimensional sliding of a layer of snow of constant thickness,  $D$ , on a base of constant slope,  $\phi$ .

[8] The stratigraphy of the dry snow slab always consists of a relatively thick strong (and stiff) slab on top of a weaker thin layer which fails in shear. Normally, the material below the weak layer is stronger (and stiffer) than that in the weak layer. In this paper, it is assumed that the snow below the weak layer is rigid, to simplify the analysis. In some cases, this is a very good assumption. This is especially true when the fracture develops over a stiff crust or ice layer.

[9] This simplifying assumption is not always completely justified but the general conclusions of the paper will not be affected by it. Thus, in general, the snow slab stratigraphy is such that shear failure initiates in the weak layer beneath the slab and then ultimately the failure becomes a rapid self-propagating shear fracture (modes II and III) within the weak layer [*McClung*, 1981]. In this paper, we consider slab avalanche initiation from the perspective of mode II fracture propagation, but extension to include mode III would be possible.

[10] For cohesive snow failing in shear, the snow is characterized as a pressure sensitive, dilatant, strain-softening material with significant rate- and temperature-dependent characteristics. In this paper, shear failure and shear fracture within the weak layer are analyzed from the perspective of LEFM assuming the slab above is elastic. However, these assumptions (elastic slab and strain-softening failure of a weak layer) require qualifiers for both the slab deformation model and weak layer failure, as explained in the following.

## 2. Assumed Slab Behavior

[11] Under most conditions for which snow slabs get released (excluding application of explosives), the snow slab (as distinct from the weak layer) will be undergoing viscoelastic deformation. The viscoelastic behavior per se nevertheless cannot be the cause of fracture because, in the field, the rates of creep deformation leading to failure are typically 2 orders of magnitude lower than necessary to achieve strain-softening behavior.

[12] Striving for simplicity, we assume in this study that the slab behaves elastically when it is failing. Since, during failure, the slab rapidly releases energy and thus undergoes fast unloading, this seems not to be a bad assumption. The problem seems similar to what is obtained in concrete which, too, exhibits strong creep yet the creep effect in fracture is not major [*Bažant and Li*, 1997]. An extension to

viscoelastic behavior, probably similar to that presented for concrete, might nevertheless be needed in future studies, for a completely realistic model. In this extension, one would need to take into account the fact that aside from viscoelasticity in the bulk of snow, the fracture in the weak layer must also be rate-sensitive and that this rate sensitivity is of a different kind than the bulk viscoelasticity [*Bažant and Li*, 1997].

[13] Alpine snow, in similarity to other geomaterials, displays different shear failure characteristics, depending on the precise loading and deformation [e.g., *McClung*, 1981, 1987]. In the literature, one finds distinctions between the “load-controlled” and the so-called “strain-controlled” conditions. The former, which is also called the “direct action,” refers to fracture during progressive snow accumulation. The latter of course does not mean that the strain would actually be controlled (which is impossible) but simply refers to “delayed action,” meaning fracture after a storm. From the fracture mechanics viewpoint, the only distinction can be between load-controlled and displacement-controlled fractures, however, the difference between them occurs only for the postpeak load-softening response, while the triggering of an avalanche must occur at the peak of the load-displacement curve. As long as the avalanche is driven by the gravity of snow, whether or not accumulating, the failure is always load controlled, while a displacement control of an avalanche is hard to imagine. As for the snow properties for fracture at snow accumulation and for delayed fracture, they can of course be quite different.

[14] It must be emphasized, however, that both types of behavior are governed by the same material laws, the only difference being in the age effect on snow properties, and probably in the deformation rates produced by the different types of loading and in the conditions of stability of equilibrium of the whole specimen or structure [*Bažant and Cedolin*, 1991]. The gradual strain-softening with dilatancy in the weak zone of course takes place under load control as well, but only after stability has been lost and the failure has become dynamic. Assuming that no prescribed displacements are applied to the snow slab, all the loading is by gravity, i.e., by the accumulated weight of the snow slab. This corresponds to the load control conditions, for which the load during failure remains approximately constant. Such conditions, along with an approximately constant deformation rate, were implicitly assumed in the classical cohesive fracture analysis of *Palmer and Rice* [1973] and will be also assumed in this study. It is further assumed that the effects of inhomogeneity and anisotropy of the snow slab can be neglected in elastic fracture analysis, and that the strain can be considered small.

## 3. Analysis by LEFM

[15] We assume that a sliding (mode II) crack of length  $2a$  develops in snow near the underlying rigid base and propagates symmetrically at both tips (Figure 1). Consider first that the residual shear stress,  $\tau_r$ , that develops in this sliding crack after large slip is negligible,  $\tau_r \approx 0$ . By arguments of symmetry, the longitudinal normal stress,  $\sigma$ , in the sliding layer must vanish at the point of symmetry, i.e.,  $\sigma \approx 0$  at  $x = 0$ , where  $x$  is the longitudinal coordinate measured from the center of the crack. The equilibrium

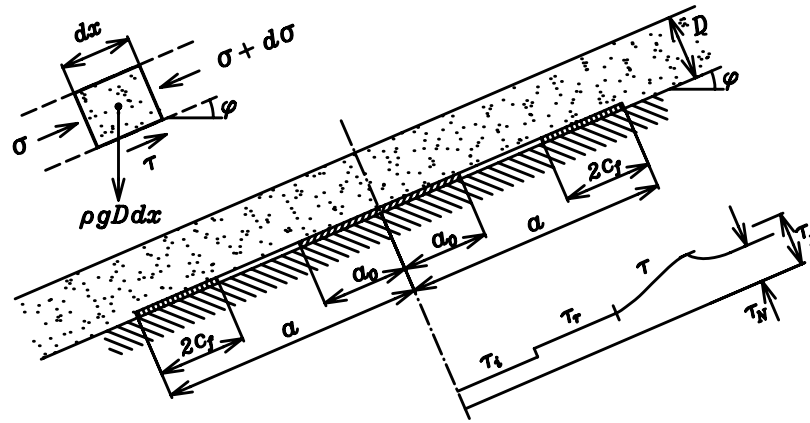


**Figure 1.** Geometry of snow slab ( $2a_0$  is initial weak zone,  $2a$  is cohesive crack,  $2c_f$  is the fracture process zone); forces acting on an element of slab (top left); and typical shear stress distribution obtained by the cohesive crack analysis (bottom right).

condition of an element  $dx$  of the layer requires that  $(\sigma + d\sigma)D - \sigma D - \rho g D dx \sin \phi = 0$  or  $d\sigma/dx = \rho g \sin \phi$  (for  $\tau = 0$ , Figure 1), which means that

$$\sigma = \rho g x \sin \phi, \quad (1)$$

where  $D$  is snow thickness and  $\rho$  is the mass density of snow (both assumed to be uniform and equal to the means calculated from thickness and density data) and  $g$  is magnitude of gravity acceleration. Beyond the crack ( $x > a$ ),  $\sigma = 0$ , and the weight of the snow slab is transmitted to the base entirely by shear stresses. Longitudinally, the upper half of the sliding layer is in tension and the lower half in compression. Evidently, a tensile break must eventually occur in the upper half, but it seems reasonable to assume that this usually happens only after stability loss and is not what triggers the avalanche [McClung, 1981].

[16] The complementary strain energy of one half of the sliding layer is

$$\Pi^* = \int_0^a \frac{\sigma^2}{2E'} D b dx = (\rho g \sin \phi)^2 \frac{Da^3 b}{6E'} = \frac{\tau_N^2 a^3 b}{6E'D}. \quad (2)$$

Here  $E'$  is the effective Young's modulus of the sliding snow layer,  $b$  is the lateral width of this layer, and  $\tau_N$  is the nominal shear stress, defined as the shear stress that would be needed to support the weight of the sliding layer if there were no crack, i.e.,

$$\tau_N = \rho g D \sin \phi. \quad (3)$$

The nominal stress,  $\tau_N$ , is a load parameter and represents the component, in the direction of slope, of the gravity force per unit base area. The energy release rate,  $\mathcal{G}$ , is

$$\mathcal{G} = \frac{1}{b} \frac{\partial \Pi^*}{\partial a} = \frac{\tau_N^2 a^2}{2E'D}. \quad (4)$$

In LEFM, the fracture criterion is  $\mathcal{G} = G_{II}$ , where  $G_{II}$  is the mode II fracture energy of snow, i.e., the energy required to

form a sliding crack of a unit area, considered as a material constant. Setting  $\mathcal{G} = G_{II}$ , one gets nominal stress at failure

$$\tau_N = \frac{\sqrt{2E'G_{II}}}{\alpha} \frac{1}{\sqrt{D}} \quad \alpha = \frac{a}{D}. \quad (5)$$

Here  $\alpha$  is the relative crack length, which will be discussed later. From now on,  $\tau_N$  will denote nominal shear strength.

[17] From experience with other size effect problems [Bažant and Planas, 1998], one may expect  $\alpha$  to be constant when geometrically similar structures of different sizes  $D$  are compared. Under that assumption, the LEFM size effect according to (5) is  $\tau_N \propto D^{-1/2}$ , which must have been expected for more fundamental reasons [Bažant, 1984, 1993]. The approximate size independence of  $\alpha$  will be better justified later.

#### 4. Approximate Nonlinear Fracture Mechanics by Equivalent LEFM

[18] The main consequence of nonlinear fracture behavior is that the fracture process zone has a certain finite length. This may be approximately taken into account by LEFM provided that the tip of an equivalent LEFM crack is assumed to lie ahead of the actual crack tip at a certain distance  $c_f$ , which is approximately constant (independent of  $D$ ) and represents about one half of the fracture process zone length.

[19] It is useful to check first the asymptotic behavior in two extreme cases. The size effect of nonlinear fracture mechanics must follow the LEFM size effect if the structure is so large that the finite fracture process zone is negligible compared to  $D$  and may be considered in relative coordinates as a point. On the other hand, at very small sizes, the size of the fracture process zone is of the same order of magnitude as  $D$ , in which case the size effect is the same as in plasticity, i.e., is absent. Therefore the size effect curve in the plot of  $\log \tau_N$  versus  $\log D$  must represent a transition between a horizontal asymptote corresponding to plasticity and the LEFM size effect given by an asymptote of slope  $-1/2$ . A formula for this transition is easily obtained from

an asymptotic series expansion of the energy release function (4) in terms of powers of  $1/D$ . Writing equation (5) as  $\tau_N = \sqrt{2EG_{II}/\alpha^2 D}$ , replacing  $\alpha^2$  with  $(\alpha_0 + c_f/D)^2$ , and taking only the first two terms of the Taylor series expansion of  $\alpha^2$  with respect to  $c_f/D$ , one obtains

$$\tau_N = \frac{\tau_0}{\sqrt{1 + D/D_0}} \quad (6)$$

where

$$\tau_0 = \sqrt{\frac{E'G_{II}}{\alpha_0 c_f}} \quad D_0 = \frac{2c_f}{\alpha_0} \quad (7)$$

Note that the plot of  $\log \tau_N$  versus  $\log D$  according to equation (6) approaches a horizontal asymptote as  $D/D_0 \rightarrow 0$ , which means that the size effect disappears and the scaling of plasticity is approached. This would not be the case if more than two terms of the series expansion of  $\alpha^2$  were retained. Keeping just two terms provides a proper asymptotic matching, with correct asymptotic behavior for both  $D/D_0 \rightarrow \infty$  and  $D/D_0 \rightarrow 0$ .

[20] Equation (6) may be recognized as the standard form of the size effect law proposed by Bažant [1984] and later supported by general asymptotic arguments [Bažant, 1997, 1999, 2002; Bažant and Chen, 1997; Bažant and Planas, 1998];  $\tau_0$  and  $D_0$  are considered as constants, which will be justified later. The dependence of the transitional size  $D_0$  on  $\alpha_0$  introduces the effect of failure geometry.

[21] The fracture energy,  $G_{II}$ , represents, in the sense of the cohesive crack model, the area under the stress-displacement curve of the cohesive shear stress,  $\tau$ , versus the sliding displacement [Rice, 1968]. For the sake of simplicity, this curve may be assumed to be linear, and then  $G_{II} = \tau_f w_f/2$ , where  $\tau_f$  is the shear strength of the layer and  $w_f$  the slip needed to reduce  $\tau$  to the residual stress  $\tau_r$ .

## 5. Generalization for Finite Residual Shear Stress, $\tau_r$

[22] When  $\tau_r > 0$  (Figure 2), two solutions must be superposed: (1) The plasticity solution for a uniform shear stress  $\tau_r$  at the sliding base, which simply is  $\tau_N = \tau_r$  and (2) the fracture mechanics solution for an appropriately defined fracture energy,  $G_{II}$ . This yields

$$\tau_N = \frac{\tau_0}{\sqrt{1 + D/D_0}} + \tau_r \quad (8)$$

As shown by Rice [1968] and Palmer and Rice [1973] by means of J integral, the fracture energy  $G_{II}$  must be interpreted, in the sense of the cohesive crack model, as the area between the stress displacement curve and the line  $\tau = \tau_r$  (Figure 2).

## 6. Asymptotic Case of Very Short Crack

[23] The foregoing one-dimensional solution is obviously asymptotically exact for  $\alpha = a/D \gg 1$ . For  $\alpha < 1$ , it is not applicable, not even approximately. For values of  $\alpha$  near 1, an accurate solution must be two-dimensional, which would

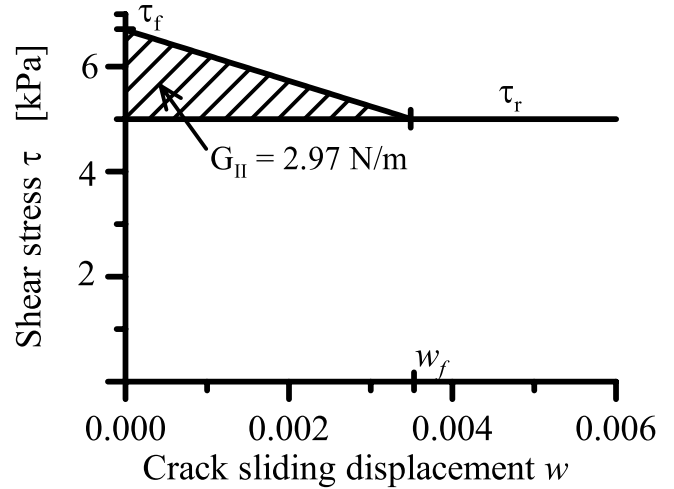


**Figure 2.** Linear softening curve assumed for cohesive crack model ( $\tau_f$  is shear strength,  $\tau_r$  is residual shear stress,  $w_f$  is critical sliding displacement; hatched area represents mode II fracture energy).

be more difficult. However, it is easy to deal with the small size asymptotic case of  $\alpha \ll 1$ . In that case, the mode II stress intensity factor must be

$$K_{II} = \tau_N \sqrt{k_2 a}, \quad (9)$$

where  $k_2$  is a dimensionless constant (with a magnitude of the order of 1).

[24] If the crack were surrounded by an infinite homogeneous space,  $k_2$  would be equal to  $\pi$ . Since the base is rigid,  $k_2$  has a different value, but we will not need to know it. The energy release rate of the small crack is  $\mathcal{G} = K_{II}^2/E''$ , where  $E''$  is a certain effective modulus value reflecting the fact that the crack lies at, or near, a rigid-elastic interface. Substituting for  $K_{II}$  and setting  $G = G_{II}$ , we obtain for the nominal strength the expression

$$\tau_N = \sqrt{E^* G_{II}/a} \quad \alpha = a/D \ll 1, \quad (10)$$

where  $E^* = E''/k_2$  is the material constant having the meaning of an adjusted Young's modulus. An approximate smooth expression for the entire range of  $D$  could be obtained by asymptotic matching of equations (5) and (10), but this avenue does not seem profitable.

## 7. Question of Crack Length at Failure

[25] The question of crack length when an avalanche is triggered may first be considered from the viewpoint of LEFM. Note that both for  $a \ll D$  and for  $a \gg D$ , the energy release rate  $\mathcal{G} = K_{II}^2/E'$  is increasing as  $a$  is increasing. In this case, called the positive geometry, the failure occurs as soon as a discrete continuous crack starts to propagate. Because, in LEFM, the fracture process zone is a point, it is already formed while  $a \ll D$ , and so an unstable fracture would have to be triggered. However, if that were the case, a sizable continuous layer of snow could never build up on a mountain slope (physically, this follows from the fact that

huge quantities of very small imperfections always exist in alpine snowpacks). There would then be no sudden avalanches [Haefeli, 1967; Grigorian, 1975]. Hence the case  $a \ll D$  does not correspond to situations of practical interest. The fact that failure at  $a \ll D$  is not the case (evidenced by the observations of McClung [1977] and McClung and Schweizer [1999]) is one reason to infer that the fracture process zone must be large, that is,  $c_f/D$  cannot be negligible.

[26] Thus  $c_f/D$  must inevitably be at least of the order of 1 or larger. Because of positive geometry, the layer will fail as soon as

$$\alpha = a/D = k, \quad (11)$$

where  $k$  is some constant larger than 1, but probably not much larger than 1. The condition  $k > 1$  is necessary for approximate applicability of the one-dimensional solution. It means that the layer will fail as soon as the crack becomes sufficiently long to make the one-dimensional approximation valid. The value of  $k$  needs to be calibrated by field observations, although its approximate value could also be estimated on the basis of two-dimensional finite element solutions. Obviously, our one-dimensional solution can apply only for not too thick snow layers, or for layers whose length is much larger than the thickness.

## 8. Problem of Dependence of Snow Properties on Slab Thickness

[27] The size effect is theoretically defined as the effect of structure size  $D$  on the nominal strength of geometrically similar structures under the assumption that the material in all such structures is the same. This assumption, however, is not satisfied for snow slabs on mountain slopes because the weight of snow and the age of snow at the base of layer have a major effect on the properties of snow at the base. An increase of thickness, which often goes along with an increase in the age of snow at the base of slab, causes densification and enhanced bonding, which increases both Young's modulus and shear strength at the base of slab. The thickness effect on the shear strength is documented by Figure 3, which shows a bilogarithmic plot of the nominal strength  $\tau_N$  from Perla's [1976] field observations of 116 natural dry snow slab avalanches. The so-called "direct action" avalanches occurring under load controlled by accumulating new snow, and those occurring with a delay (after a storm), were not distinguished in these data, but most data probably correspond to the former type, which represents about 90% of all avalanches. Anyway, a significant difference between fracture occurring at snow accumulation (increasing load) or with a delay (constant load) can occur only in postpeak response, while the load peaks and size effect should be about the same (for the same snow properties).

[28] In view of the foregoing analysis, the fact that  $\tau_N$  in Figure 3 increases, rather than decreases, with the slab thickness  $D$  can only be explained by a strengthening effect of the slab weight on  $G_{II}$  (one might be tempted to directly attribute it to an increase of shear strength, but that would be incorrect because the triggering of avalanches is a problem of fracture and strain softening, for which the strength

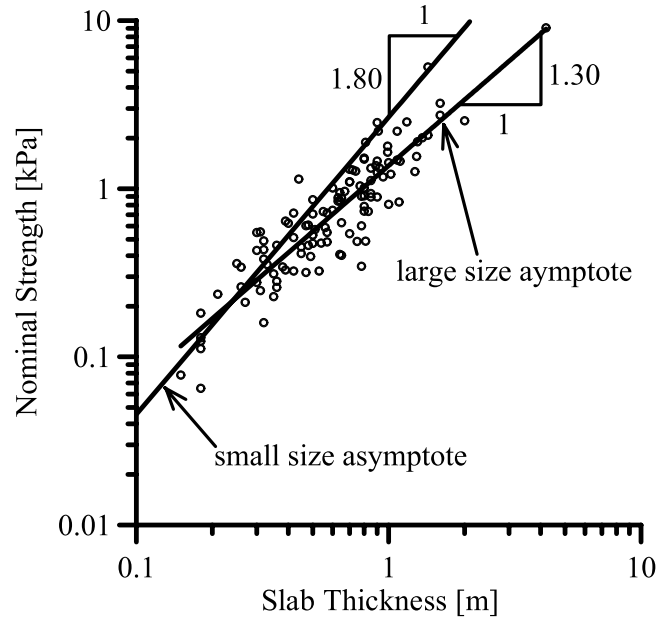


**Figure 3.** Nominal snow strength (in kPa) versus dry snow slab thickness (in m) measured for 116 avalanches [after Perla, 1976]; the regression line is  $\tau_N = 1.37 D^{1.30}$ , with  $r^2 = 0.81$  and standard error 0.37.

concept is inadequate). For this reason, we must distinguish here among (1) the structural size effect (a consequence of fracture mechanics), (2) the material size effect (caused by a change in material properties), and (3) the combined (material structural) size effect, the last being what is needed for practical applications.

[29] The trend of the data points in Figure 3 is approximately a straight line. The regression line of this set of points, shown in Figure 3, is found to have approximately the slope of 1.3, which means that the dependence of the critical value of nominal shear stress varies with the slab thickness on the average according to the power law:

$$\tau_N = C_1 D^{1.30}, \quad (12)$$

where  $C_1 = 1.37 \text{ kPa/m}^{1.3}$ . According to equations (7) and (8), the large-size asymptotic structural size effect is

$$\tau_N = \frac{1}{\alpha_0} \sqrt{\frac{2E'G_{II}}{D}} + \tau_r \quad D \gg c_f. \quad (13)$$

Equating equations (12) and (13) for  $\tau_N$  and neglecting  $\tau_r$ , we get a simple power law for the thickness effect on the fracture toughness at the base of snow slab:

$$K_{IIc} = \sqrt{E'G_{II}} = (\alpha_0 C_1 / \sqrt{2}) D^{1.80} \quad D \gg c_f, \quad (14)$$

where  $K_{IIc}$  represents the mode II fracture toughness. If  $\tau_r$  were taken into account, this relation would no longer be a power law, that is, the plot in Figure 3 would not be a straight line; but the scatter width of data points is too broad to judge any deviation from a straight line.

[30] The small-size asymptotic structural size effect according to equations (7) and (8) is  $\tau_N = \tau_0 = (EG_{II}/\alpha_0 c_f)^{1/2} = \text{const}$  (i.e., no size effect), if  $\tau_r$  is again neglected. Inserting here the material property variation in equation (14), we conclude that  $\tau_N = C_0 D^{1.80}$ , where  $C_0 = \sqrt{\alpha_0/2c_f}$ . This power law corresponds to the straight line of slope 1.80 plotted in Figure 3 (with  $C_0 = 2.67$ ), which is seen to roughly match the initial small-size trend of the data in Figure 3. Now it should be noted that the regression line of all the points for  $D < 0.35$  m (not plotted in Figure 3) is found to have the slope of 1.76. The fact that 1.76 is close to 1.80, the initial regression slope deduced from the size effect law, may be seen as a further support (albeit not a proof) of the fact that the size effect on  $\tau_N$  represents a gradual transition from the case of no size effect ( $\tau_N \propto D^0 = \text{const.}$ ) to the LEFM size effect ( $\tau_N \propto D^{-1/2}$ ). Conversely, if the initial regression slope were very different from 1.80, and especially if it were less than 1.30, it would be an argument against the present theory.

[31] So we see that there exists a certain material property variation (equation (13)) that leads to a reasonable match of the field observations with the present theory (because of the large scatter in Figure 3, it is not possible to determine from this comparison the value of  $\tau_r$ , which is therefore neglected). However, the acceptable agreement in Figure 3 is not a proof of the theory. We have not demonstrated that the same data could not be fit equally well by some other theory. Doubtless they could, since we possess only one type of data among many types that might be desired. Especially, measurements of the dependence of the snow properties on the thickness of the snow slab will be needed. Only then the present theory can be experimentally verified. For this reason, we will now offer another theoretical support for the present size effect theory based on the cohesive crack model.

## 9. Numerical Verification of Size Effect Law by Cohesive Crack Model

[32] *Hillerborg et al.* [1976], *Hillerborg* [1985], and *Petersson* [1981] analyzed mode I cohesive fracture by condensing out all the nodes other than those on the crack line and at the load point from the structural stiffness matrix. Thus they obtained the compliance matrix for the crack surface nodes and the load point [see also *Bažant and Planas*, 1998]. The governing equations were then obtained from the crack compatibility condition.

[33] In the present problem of mode II fracture with a finite residual stress, the condition of compatibility of the crack opening with the deformation of the layer of snow may be written in a dimensionless form as [*Zi and Bažant*, 2003]:

$$\bar{w}(\xi) = -\bar{D} \int_{\alpha_i}^{\alpha} \bar{C}(\xi, \xi') \bar{\tau}(\xi') d\xi' - \bar{D} \bar{\tau}_i \bar{C}^i(\xi) + \bar{D} \bar{\tau}_N \bar{C}^N(\xi), \quad (15)$$

which must be coupled with the condition that the stress intensity factor at the cohesive crack tip  $K_{II} = 0$ ; here  $\xi = x/D$  is dimensionless coordinate,  $\bar{D} = \tau_f D / E w_f = D / 2l_{ch}$  is dimensionless size ( $l_{ch}$  is Irwin's characteristic length),  $\bar{w} = w/w_f$  is dimensionless crack sliding displacement,  $\bar{\tau} = \tau/\tau_f$  is dimensionless shear stress,  $\alpha_i = a_i/D$  is dimensionless length

of the weak zone (acting as a notch),  $\bar{C}^N = C^N E/D$  is dimensionless compliance corresponding to the nominal stress  $\bar{\tau}_N = \tau/\tau_N$ ,  $\bar{C}^i = C^i E/D$  is dimensionless compliance corresponding to preexisting stress  $\bar{\tau}_i = \tau_i/\tau_f$  on the weak zone, and  $\bar{C} = E/C$  is dimensionless compliance for stress in fracture process zone; i.e.,  $\bar{w}$  at  $\xi$  caused by unit stress  $\bar{\tau}$  at  $\xi'$  ( $C^N$ ,  $C^i$ , and  $C$  are actual compliances). Note that all the variables in equation (15) are dimensionless.

[34] In *Hillerborg's* [1985] and *Petersson's* [1981] approach, the crack compatibility condition of the type of equation (15), coupled with the condition  $K_{II} = 0$ , is integrated in small loading steps, which means that the entire history of displacement distributions must be followed even though only the peak load is needed. In the case of size effect studies, the entire histories of displacement distributions must be computed for many different sizes.

[35] *Li and Liang* [1993], *Li and Bažant* [1997] and *Li and Bažant* [1994] (in a discrete form), and *Bažant and Li* [1995] (in a continuous form), developed for size effect studies a more efficient procedure in which the deformation history need not be computed and the peak load is calculated directly [see also *Bažant and Planas*, 1998, section 7.5.4]. In this procedure, the problem is inverted by searching for the size  $D$  for which a given relative crack length  $\alpha$  corresponds to the peak load (or to  $\tau_N$ ). For the present problem, this solution procedure must be adapted from mode I to mode II fracture, which is quite easy. It must also be generalized for nonzero residual stress  $\tau_r$ . The way to do that [*Zi and Bažant*, 2003] is sketched in Appendix A.

[36] In this approach, the problem of directly calculating  $\tau_N$  for various  $D$ , without solving the history of displacement distribution, is recast as an eigenvalue problem. The size  $D$  for which a given  $\alpha$  corresponds to the peak load is the eigenvalue in the following dimensionless homogeneous Fredholm integral equation:

$$\bar{w}_{,\alpha}(\xi) + \bar{D} \int_{\alpha_i}^{\alpha} \bar{C}(\xi, \xi') \bar{\tau}_{,\bar{w}} \bar{w}_{,\alpha}(\xi') d\xi' = 0, \quad (16)$$

in which the subscripts preceded by a comma denote partial derivatives. Equation (16) is almost the same as that of *Bažant and Li* [1995, equation (9)] except that  $\bar{\tau}_{,\bar{w}}$  is used instead of  $\bar{w}_{,\bar{\tau}}$  (this is more generally applicable to crack propagation problems in which the slope of the energy release rate changes from negative to positive [*Zi and Bažant*, 2003]). The peak load is characterized by the nominal strength calculated from

$$\bar{\tau}_N = \frac{\int_{\alpha_i}^{\alpha} \bar{w}_{,\alpha}(\xi) d\xi + \bar{D} \bar{\tau}_i \int_{\alpha_i}^{\alpha} \bar{C}^i(\xi) \bar{w}_{,\alpha}(\xi) d\xi}{\bar{D} \int_{\alpha_i}^{\alpha} \bar{C}^N(\xi) \bar{w}_{,\alpha}(\xi) d\xi}. \quad (17)$$

[37] Choosing a series of  $\alpha$  values, one solves for each of them the eigenvalue  $\bar{D}$  as well as the eigenmode  $\bar{w}_{,\alpha}$  (approximated as an eigenvector) from a discrete approximation of equation (16). Knowing  $\bar{D}$  and  $\bar{w}_{,\alpha}$ , one may then simply evaluate  $\bar{\tau}_N$  from the discrete approximation of equation (17).

[38] The snow layer in Figure 1 is considered as an example. The values  $E = 987.5$  kPa, Poisson ratio  $\nu = 0.25$ ,  $\tau_f = 6.7$  kPa,  $\tau_r = 5.0$  kPa, and  $w_f = 3.5$  mm are chosen as the typical values for snow (based on the work by *McClung*

[1977, 1979]). The crack line is subdivided by nodes into many equal intervals (Figure 4). The discrete values of the compliance  $\bar{C}(\xi, \xi')$  are computed by condensing out the interior nodes from a two-dimensional finite element analysis in the vertical plane (Figure 4), assuming the plane strain condition. To take into account the infinite length of the snow slab, the so-called “soak” elements (elements taking into account the effect of an infinite layer) are used at the ends of the meshed domain in computing the compliance.

[39] The nominal strength values computed by the eigenvalue analysis are plotted in Figure 5a for two initial weak zone lengths  $a = 5D$  and  $10D$ . As one can see, the trend of  $\log \tau_N$  versus  $\log D$  reveals a size effect. This trend can be closely fit by equation (8).

[40] To fit the size effect law (8) to the values obtained by the numerical cohesive crack analysis, it is convenient to rearrange equation (8) as a linear plot of  $\tau^{-2}$  versus  $D$  (where  $\tau = \tau_N - \tau_r$ , Figure 5b), given by

$$\frac{1}{(\tau_N - \tau_r)^2} = \frac{1}{\tau_0^2} + \frac{1}{\tau_0^2 D_0} D. \quad (18)$$

Choosing various values of  $\tau_r$ , one can pass a regression line of  $Y = (\tau_N - \tau_r)^{-2}$  versus  $X = D$ . The  $Y$  intercept of this line is  $\tau_0^{-2}$  and its slope is  $(1/\tau_0^2 D_0)$ , from which the optimum values of cohesive strength of the material,  $\tau_0$ , and of the transitional size  $D_0$  may be identified (Figure 5b) for each  $\tau_r$ . The optimum value of  $\tau_r$  is that which gives the smallest coefficient of variation of errors. Then, using equation (7), one may calculate the fracture energy  $G_{II} = \alpha_0 c_f \tau_0^2 / E$  and the half length of fracture process zone,  $c_f = \alpha_0 D_0 / 2$ . The  $G_{II}$  value must, of course, approximately agree with the shaded area in Figure 2, which is  $G_{II} = 2.97$  N/m. The longer the initial weak zone, the better is the agreement of the input and output values of  $G_{II}$ .

## 10. Effect of Preexisting Finite Weak Zone at Snow Base

[41] A cohesive snow slab, often packed by strong winds [McClung and Schaerer, 1993], is delimited at its base a

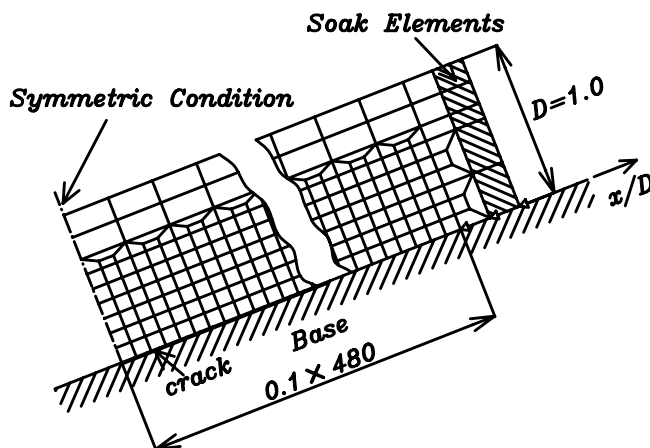
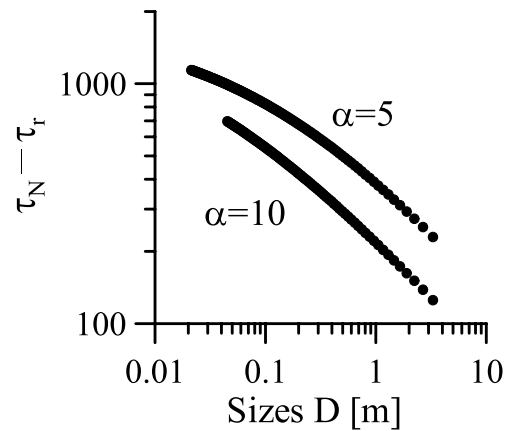
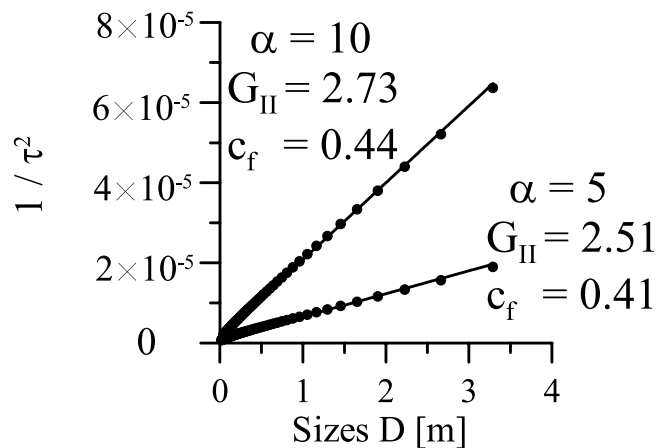


**Figure 4.** Two-dimensional finite element mesh from which crack node compliance matrix is computed (line of symmetry, dash-dotted, is at left, and crack at base propagates to the right).



(a)



(b)

**Figure 5.** (a) Size effect curve obtained by eigenvalue analysis of cohesive crack model based on two-dimensional finite elements. (b) Linear regressions (for optimum  $\tau_r$ ) used to identify fracture parameters via size effect law deduced.

weak layer that acts as a preexisting notch from which shear crack propagation initiates. Natural macroscopic imperfections [McClung and Schaerer, 1993] are thought to be the main source of such preexisting layer.

[42] The efficient eigenvalue approach is now insufficient because it skips the calculation of the load-displacement curve and the stress distribution. Therefore we now use Hillerborg *et al.*'s [1976], Hillerborg's [1985], and Petersson's [1981] classical incremental loading approach based on the compliance matrix for crack line nodes. Three cases,  $\tau_i/\tau_r = 0.50, 0.75,$  and  $1.00$ , are plotted. The weak zone length is assumed to be  $a = 10D$  for every case, which preserves geometric similarity (otherwise we could not isolate the size effect from the geometry effect). The computed stress profiles along the crack line are plotted in Figure 6 for snow thickness  $D = 0.1$  m, and the evolutions of the nominal stress  $\tau_N$  with the increasing relative (dimensionless) crack length  $\alpha$  are plotted in Figure 7. Of course,  $\tau_i$  can be greater than  $\tau_r$ , but it would be make no

sense to analyze such situations because  $\tau_i$  must get reduced to  $\tau_r$  before the shear crack develops.

[43] An interesting property is found. Normally, stable fracture propagation terminates with some kind of unstable softening response, that is, there exists a peak load followed by such softening. However, among the three calculated results, this is true only for  $\tau_i/\tau_r = 1.00$ . For  $\tau_i/\tau_r = 0.50$  and  $0.75$ , there is no peak, and no post peak softening. This, of course, means that for  $0.50$  and  $0.75$ , there is no size effect either. So, for a given  $D$ , there must exist certain critical values  $\tau_{cr}$  such that for  $\tau_i < \tau_{cr}$ , no catastrophic (dynamic) failure develops according to the assumptions of the present analysis. The value of  $\tau_{cr}$  will of course depend not only on  $D$  but also on  $a_i/D$ .

[44] To clarify this behavior, note that stress concentrations at the front of an existing crack may cause the residual strength  $\tau_r$  to be exceeded locally even if the average shear stress represented by  $\tau_N$  is less than  $\tau_r$ . For this special case, the shear crack grows under an increasing load, i.e., increasing  $\tau_N$  (the increase of load being necessary to make the energy release rate equal to the fracture energy). This is a stable crack growth, and so a softening response, which would cause stability loss and trigger an avalanche, is never reached, provided that  $\tau_r$  is assumed to be uniform along the slab and the normal stress  $\sigma$  in Figure 1 is less than the strength limit for normal stress. In practice,  $\tau_r$  would randomly fluctuate, and then of course a point of stability loss may be reached (this kind of behavior may explain why sometimes an avalanche may release only after a number of skiers have crossed the same slope on the same track).

[45] What is the mathematical reason that the softening and unstable fracture propagation occur only for  $\tau_i > \tau_{cr}$ ? This can be explained analytically by LEFM. The complementary energy and the corresponding energy release rate of a half layer of the snow slab in Figure 1 is, in the one-dimensional approximation,

$$\begin{aligned} \Pi^* = & \frac{D}{2E'} \left[ \int_0^{a_i} \left\{ (\tau_N - \tau_i) \frac{x}{D} \right\}^2 dx \right. \\ & \left. + \int_{a_i}^a \left\{ (\tau_N - \tau_r) \frac{(x - a_i)}{D} + (\tau_N - \tau_i) \frac{a_i}{D} \right\}^2 dx \right] \end{aligned} \quad (19)$$

$$\mathcal{G} = \frac{\partial \Pi^*}{\partial a} = [(\tau_N - \tau_r)\alpha + (\tau_r - \tau_i)\alpha_i]^2 \frac{D}{2E'}, \quad (20)$$

where  $a_i$  is the half length of the initial weak zone and  $\alpha_i = a_i/D$ . Note that here it is necessary to distinguish  $a_i$  (or  $\alpha_i$ ) from  $a$  (or  $\alpha$ ) because the stress on the slip surface which is generated by propagation is equal to  $\tau_r$ . Equating  $\mathcal{G}$  to the fracture energy  $G_{II}$ , one obtains the expression of the nominal strength:

$$\tau_N - \tau_r = \frac{\sqrt{2E'G_{II}}}{\alpha\sqrt{D}} - (\tau_r - \tau_i) \frac{\alpha_i}{\alpha}. \quad (21)$$

Equation (21) is plotted in Figure 8a for two different sizes  $D$ . Both curves asymptotically approach the zero line. The top (decreasing) curve exhibits a size effect, while the bottom (increasing) curve does not. The critical condition

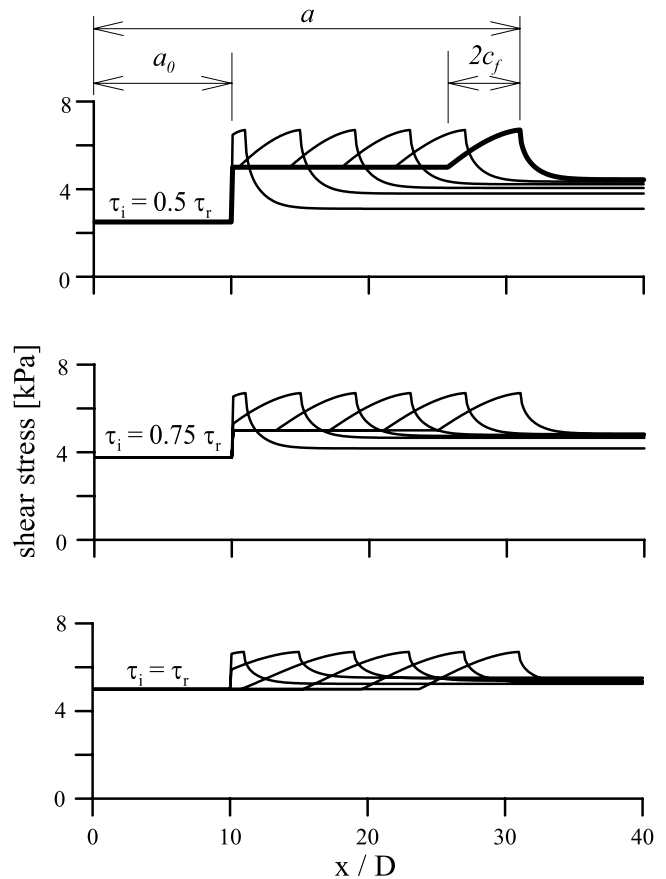


**Figure 6.** Stress profiles along the base for three different values of  $\tau_i$  in initial weak zone.

for the transition between them is  $\tau_N - \tau_r = 0$ . So the critical depth and the critical stress  $\tau_{cr}$  in the weak zone are

$$D_{cr} = \frac{2E'G_{II}}{a_i^2(\tau_r - \tau_i)^2} \tau_{cr} = \tau_r - \frac{\sqrt{2E'G_{II}}}{a_i\sqrt{D}}. \quad (22)$$

When  $D < D_{cr}$  or  $\tau_i > \tau_{cr}$ , a fracturing snow slab will exhibit postpeak softening. Its nominal strength  $\tau_N$  will exceed  $\tau_r$  and will be characterized by a size effect. Otherwise,  $\tau_N$  will never exceed  $\tau_r$ , no size effect will exist, and the asymptotic nominal strength  $\tau_N$  will be the residual strength of the weak layer  $\tau_r$ .

[46] Equation (20) also provides a simple explanation why a size effect exists. For similar cracks ( $\alpha = \text{const}$ ) and the same  $\tau_N$ , the energy release rate increases with  $D$ , while the energy dissipation rate  $\mathcal{G}$  is constant,  $\mathcal{G} = G_f$ . Thus energy balance is possible only if  $\tau_N$  decreases with  $D$ . The same intuitive explanation applies to all kinds of deterministic size effect in failure preceded by a large stable crack growth [Bažant and Chen, 1997; Bažant, 2002].

[47] To estimate the critical values  $D_{cr}$  and  $\tau_{cr}$  for our example, we may interpolate the results for  $\tau_i/\tau_r = 0.5, 0.75$ , and  $1.0$ . To this end, we may plot the difference  $\tau_{40} - \tau_{15}$ , where  $\tau_{15} = \tau_N - \tau_r$  for  $x/D = 15$  and  $\tau_{40} = \tau_N - \tau_r$  for  $x/D = 40$  as plotted in Figure 8b. From Figure 8b, one gets

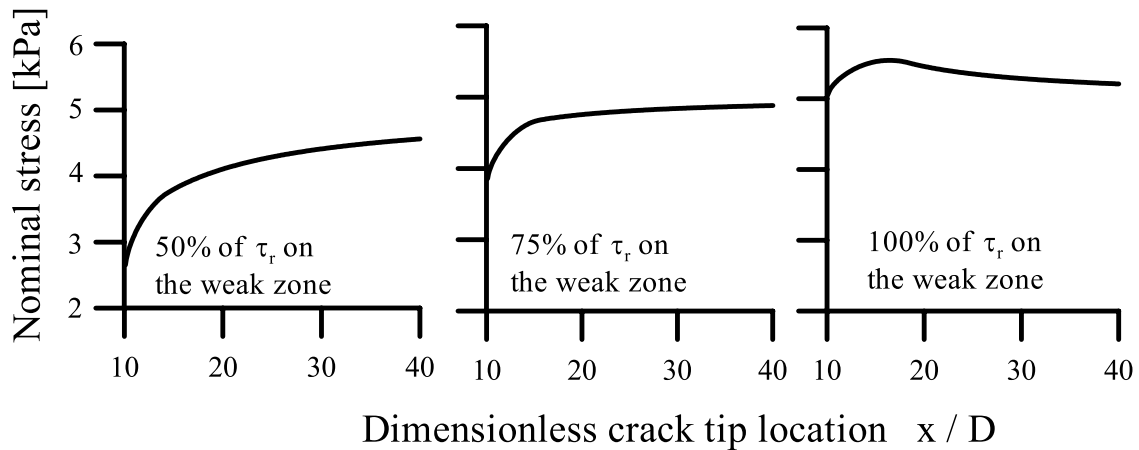


**Figure 7.** Nominal stress evolutions calculated by the cohesive crack model as shear crack propagates, for three different values of preexisting stress  $\tau_i$  in initial weak zone.

the critical point  $\tau_{cr} = 0.85\tau_r$ . The same value is obtained by equation (22).

### 11. Possible Ramifications: Mud, Clay, or Rock Slides

[48] Before closing, it should be pointed out that the usual strength-based infinite slope model for landslide failures, which has been prevalent in engineering texts for more than fifty years, will not apply for strain-softening materials including rock joints and clay slides. The present analysis of fracture and size effect may be applicable without major modifications to any sudden failure of natural slopes, such as mud slides, clay slides, and rock slides, provided that the material is quasi-brittle, characterized by strain softening.

[49] Similar to snow slabs, a weak layer typically occurs in mud or clay slope. The weak layer can be a previously fractured zone, a slippery interface at base, or a zone

weakened by water. In this weak layer, the preexisting initial shear stress  $\tau_i$  can be smaller than  $\tau_r$ .

### 12. Conclusions

1. Whereas the size effect is theoretically defined as the dependence of nominal strength on structure size for the same material properties, in nature the snow slabs of different thicknesses have very different properties at their base. Therefore one must distinguish between the structural size effect and the material size effect. The combined size effect applicable to avalanches must be obtained by modifying the structural size effect law according to the thickness dependence of material properties. The structural size effect cannot be directly measured and must be obtained theoretically. To obtain the material size effect experimentally, one must match the data on the effect of snow thickness with the combined size effect law.

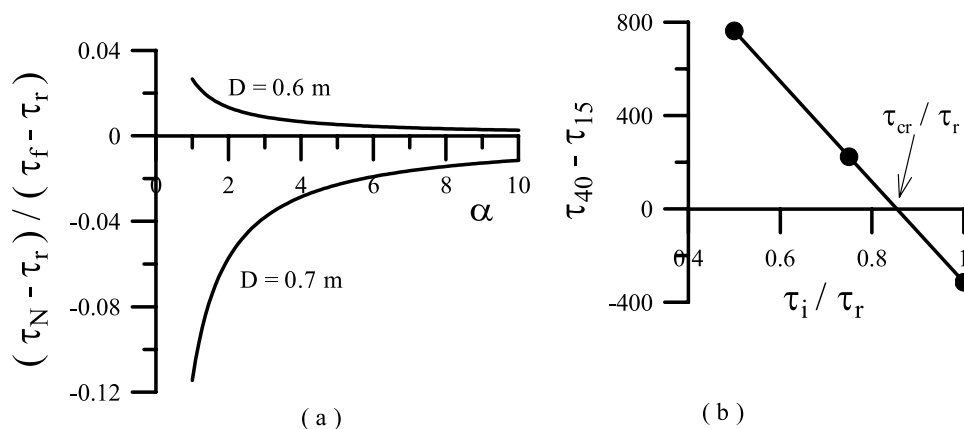


**Figure 8.** Effect of the preexisting finite weak zone on the nominal strength of snow slab. (a) The hardening nominal stress (bottom curve) compared to the softening nominal stress (top curve) as the crack propagates, and (b) interpolation to identify the critical preexisting stress in equation (22) along the weak zone.

2. The failure of a snow slab, which is a nonlinear fracture mechanics problem previously discussed in terms of the cohesive crack model, can be approximately described by equivalent LEFM, with the shear (mode II) fracture energy  $G_{II}$  and the effective half length of the fracture process zone,  $c_f$ , as the basic parameters. If the snow layer is thicker than the fracture process zone, a one-dimensional solution is acceptable. The equivalent LEFM solution becomes close to the numerical solution for the cohesive crack model as the notch length increases.

3. Equivalent LEFM yields a simple formula for the theoretical size effect, identical to the size effect law introduced by *Bažant* [1984] for concrete and quasi-brittle materials in general. This formula is in a one-to-one relationship to the cohesive crack model, which means that the parameters of one can be approximately converted to the parameters of the other.

4. The failure mode depends on the preexisting shear stress  $\tau_i$  in the fracture-triggering weak zone at the base of snow slab. There exists a critical stress  $\tau_i = \tau_{cr}$  and a critical depth  $D_{cr}$  such that for  $D > D_{cr}$  or  $\tau_i < \tau_{cr}$ , there is no structural size effect, no peak load, and no post peak softening. The value of  $\tau_{cr}$  is approximately 85% of the residual shear stress at the base of a sliding layer, in the case considered in this paper.

5. Because the fracture process zone is quite large, it is not easy to perform laboratory experiments simulating avalanches. Direct measurement of the size effect per se is next to impossible because the effects of snow weight and aging prevent finding different-sized samples with similar mechanical properties.

6. The modification of the structural size effect law taking into account the thickness dependence of snow properties at base may be done by replacing the constant fracture toughness and the limiting zero-size strength with quantities that increase with snow slab thickness. The existing data suggest that the increase is very strong, with the toughness increasing roughly as (snow thickness)<sup>1.8</sup>. However, the available field data are too limited to allow precise conclusions and provide experimental verification of the present theory.

7. For the sake of simplicity and clarity, the viscoelastic and thermal aspects of snow deformation have been neglected in the present analysis. Despite the general importance of these phenomena, their effect on the mechanics of snow slab fracture (like concrete fracture) is probably not very strong since the snow slab is rapidly unloading as it releases its strain energy during failure. The temperature and age, aside from snow slab thickness, have of course a large influence on the values of  $G_{II}$  and  $E'$ .

## Appendix A: Eigenvalue Analysis of the Cohesive Crack Model

[50] The condition that the stress intensity factor at the tip of the cohesive crack must vanish is

$$\int_{\alpha_i}^{\alpha} k(\xi) \bar{\tau}(\xi) d\xi + k^i \bar{\tau}_i - k^N \bar{\tau}_N = 0, \quad (A1)$$

where  $k(\xi)$  is the influence function and influence coefficients of dimensionless stress intensity factor ( $k(\xi)$ ,  $k^i(\xi)$ ),

and  $k^N(\xi)$  is the actual influence function and coefficients). Differentiating equation (15) at continuing equilibrium, we have

$$\begin{aligned} \bar{w}_{,\alpha} = & -\bar{D} \int_{\alpha_0}^{\alpha} [\bar{C}_{,\alpha}(\xi, \xi') \bar{\tau}(\xi') + \bar{C}(\xi, \xi') \bar{\tau}_{,\alpha}(\xi')] d\xi' \\ & - \bar{D} \bar{C}(\xi, \alpha) \bar{\tau}(\alpha) - \bar{D} \bar{\tau}_i \bar{C}_{,\alpha}^i(\xi) \\ & + \bar{D} \bar{\tau}_N \bar{C}_{,\alpha}^N(\xi) + \bar{D} \frac{\partial \bar{\tau}_N}{\partial \alpha} \bar{C}^N(\xi), \end{aligned} \quad (A2)$$

where the third term and the last term are recognized to be zero because of  $C(\xi, \alpha) = 0$  and the maximum load condition  $\partial \bar{\tau}_N / \partial \alpha = 0$ . Now, one can use the following well-known relations between the compliances and the stress intensity factors [e.g., *Bažant and Planas*, 1998]:

$$\frac{\partial \bar{C}^N}{\partial \alpha} = 2k(\xi) k^N \quad (A3)$$

$$\frac{\partial \bar{C}(\xi, \xi')}{\partial \alpha} = \frac{\partial}{\partial \alpha} \frac{\partial^2 \bar{\Pi}^*}{\partial \bar{\tau}(\xi) \partial \bar{\tau}(\xi')} = \frac{\partial^2}{\partial \bar{\tau}(\xi) \partial \bar{\tau}(\xi')} \frac{\partial \bar{\Pi}^*}{\partial \alpha} = 2k(\xi) k(\xi'). \quad (A4)$$

Then equation (A2) becomes

$$\begin{aligned} \bar{w}_{,\alpha} = & -\bar{D} \int_{\alpha_0}^{\alpha} \bar{C}(\xi, \xi') \bar{\tau}_{,\alpha}(\xi') d\xi' \\ & - 2\bar{D} k(\xi) \left[ \int_{\alpha_i}^{\alpha} k(\xi') \bar{\tau}(\xi') d\xi' + k^i \bar{\tau}_i - k^N \bar{\tau}_N \right]. \end{aligned} \quad (A5)$$

Thus equation (A1) leads to an eigenvalue problem expressed by the homogeneous integral equation [*Bažant and Li*, 1995; *Bažant and Planas*, 1998]:

$$\int_{\alpha_i}^{\alpha} -\bar{C}(\xi, \xi') \bar{\tau}_{,\bar{w}}(\xi') \bar{w}_{,\alpha}(\xi') d\xi' = \frac{1}{\bar{D}} \bar{w}_{,\alpha}(\xi). \quad (A6)$$

[51] The nominal strength  $\bar{\tau}_N$  can then be obtained from the crack compatibility condition (15). This condition is multiplied by  $\bar{\tau}_{,\bar{w}}(\xi) \bar{w}(\xi)_{,\alpha}$  and, upon integrating from  $\alpha_i$  to  $\alpha$ ,  $\bar{w}_{,\alpha}$  is expressed from equation (A6) and substituted into the term  $-\bar{D} \int_{\alpha_0}^{\alpha} \bar{C} \bar{\tau}_{,\bar{w}}(\xi) \bar{w}_{,\alpha}(\xi) d\xi$ , in which the symmetry property of the compliance matrix is used to interchange the integration variable  $\xi$  with  $\xi'$ . This leads to the following expression for the dimensionless nominal strength [*Bažant and Li*, 1995; *Bažant and Planas*, 1998; *Zi and Bažant*, 2003]:

$$\begin{aligned} \bar{\tau}_N = & \int_{\alpha_0}^{\alpha} \left\{ \bar{w}_{,\alpha}(\xi) [\bar{\tau}_{,\bar{w}}(\xi) \bar{w}(\xi) - \bar{\tau}(\xi)] \right. \\ & \left. + \bar{D} \bar{\tau}_i \bar{C}^i(\xi) \bar{\tau}_{,\bar{w}}(\xi) \bar{w}_{,\alpha}(\xi) \right\} d\xi \\ & / \bar{D} \int_{\alpha_0}^{\alpha} \bar{C}^N(\xi) \bar{\tau}_{,\bar{w}}(\xi) \bar{w}_{,\alpha}(\xi) d\xi. \end{aligned} \quad (A7)$$

When the softening law up to the critical sliding displacement is linear, the simpler form in equation (17) is obtained.

## Notation

$a$	crack length, m.
$b$	lateral width of sliding snow layer, m.
$c_f$	a half length of failure process zone, m.
$C$	compliance.
$\bar{C}$	dimensionless compliance.
$D$	nominal size of sliding snow slab, i.e., depth, m.
$\bar{D}$	dimensionless size of sliding snow slab.
$D_{cr}$	critical size, m.
$E'$	effective Young's modulus of sliding snow layer, Pa.
$g$	magnitude of gravity acceleration.
$G$	energy release rate, N/m.
$G_{II}$	mode II fracture energy of snow, N/m.
$i$	superscript or subscript labeling preexisting (initial) stress in the weak zone.
$K_{II}$	mode II fracture toughness of snow, $\text{N/m}^{1.5}$ .
$N$	superscript or subscript labeling nominal strength.
$w$	crack sliding displacement, m.
$\bar{w}$	dimensionless crack sliding displacement.
$w_f$	critical slip needed to reduce shear stress to the residual stress $\tau_r$ , m.
$x$	longitudinal coordinate measured from the center of crack, m.
$\alpha$	dimensionless crack length, m.
$\alpha_0$	dimensionless initial crack length, m.
$\phi$	angle of slope.
$\tau_{cr}$	critical preexisting (initial) shear stress on the crack, Pa.
$\tau_f$	shear strength, Pa.
$\tau_r$	residual shear stress, Pa.
$\tau_N$	nominal shear strength, Pa.
$\bar{\tau}$	dimensionless shear stress.
$\sigma$	longitudinal normal stress, Pa.
$\rho$	mass density of snow, $\text{kg/m}^3$ .
$\nu$	Poisson ratio.
$\xi$	dimensionless coordinate.

[52] **Acknowledgments.** The work of the first two authors was partially supported under National Science Foundation grant CMS-9713144 to Northwestern University, and the work of the third author was supported by the Natural Sciences and Engineering Research Council of Canada.

## References

- Bažant, Z. P., Size effect of blunt fracture: Concrete, rock, metal, *J. Eng. Mech.*, 110, 518–535, 1984.
- Bažant, Z. P., Scaling laws in mechanics of fracture, *J. Eng. Mech.*, 119, 1828–1844, 1993.
- Bažant, Z. P., Scaling of quasibrittle fracture: Asymptotic analysis, *Int. J. Fract.*, 83(1), 19–40, 1997.
- Bažant, Z. P., Size effect on structural strength: A review, *Ing. Arch.*, 69, 703–725, 1999.
- Bažant, Z. P., *Scaling of Structural Strength*, Hermes-Penton, London, 2002.
- Bažant, Z. P., and E. P. Chen, Scaling of structural failure, *Appl. Mech. Rev.*, 50(10), 593–627, 1997.

- Bažant, Z. P., and Y.-N. Li, Stability of cohesive crack model, part II, Eigenvalue analysis of size effect on strength and ductility of structures, *J. Appl. Mech.*, 62, 965–969, 1995.
- Bažant, Z. P., and L. Cedolin, *Stability of Structures: Elastic, Inelastic Fracture and Damage Theories*, Oxford Univ. Press, New York, 1991.
- Bažant, Z. P., and J. Planas, *Fracture and Size Effect in Concrete and Other Quasibrittle Materials*, CRC Press, Boca Raton, Fla., 1998.
- Daerr, A., and S. Douady, Two types of avalanche behaviour in granular media, *Nature*, 399, 241–243, 1999.
- Grigorian, S. S., Mechanics of snow avalanches: Snow mechanics, *IASH Publ.*, 114, 335–368, 1975.
- Haefeli, R., Some mechanical aspects on the formation of avalanches, *Phys. Snow Ice Conf. Proc.*, 1(2), 1199–1213, 1967.
- Hillerborg, A., Numerical methods to simulate softening and fracture of concrete, in *Fracture Mechanics of Concrete: Structural Application and Numerical Calculation*, edited by G. C. Sih and A. DiTomasso, pp. 141–170, Martinus Nijhoff, Zoetermeer, Netherlands, 1985.
- Hillerborg, A., M. Modéer, and P. E. Petersson, Analysis of crack formation and crack growth in concrete by means of fracture mechanics and finite elements, *Cement Concrete Res.*, 6, 773–782, 1976.
- Li, Y., and Z. P. Bažant, Eigenvalue analysis of size effect for cohesive crack model, *Int. J. Fract.*, 66, 213–226, 1994.
- Li, Y., and Z. P. Bažant, Cohesive crack with rate-dependent opening and viscoelasticity, II, Numerical algorithm, behavior and size effect, *Int. J. Fract.*, 86, 267–288, 1997.
- Li, Y.-N., and R. Y. Liang, The theory of boundary eigenvalue problem in the cohesive crack model and its application, *J. Mech. Phys. Solids*, 41(2), 331–350, 1993.
- McClung, D. M., Direct simple shear tests on snow and their relation to slab avalanche formation, *J. Glaciol.*, 19(81), 101–109, 1977.
- McClung, D. M., Shear fracture precipitated by strain softening as a mechanism of dry slab avalanche release, *J. Geophys. Res.*, 84(B7), 3519–3526, 1979.
- McClung, D. M., Fracture mechanical models of dry slab avalanche release, *J. Geophys. Res.*, 86(B11), 10,783–10,790, 1981.
- McClung, D. M., Mechanics of snow slab failure from a geotechnical perspective, in *Avalanche Formation, Movement and Effects*, IASH Publ., 162, 475–505, 1987.
- McClung, D. M., and P. Schaerer, *The Avalanche Handbook*, The Mountaineers, Seattle, Wash., 1993.
- McClung, D. M., and J. Schweizer, Skier triggering, snow temperatures and the stability index for dry-slab avalanche initiation, *J. Glaciol.*, 45(150), 190–200, 1999.
- Palmer, A. C., and J. R. Rice, The growth of slip surfaces on the progressive failure of over-consolidated clay, *Proc. R. Soc. London, Ser. A*, 332, 527–548, 1973.
- Perla, R. I., The slab avalanche, Ph.D. thesis, Univ. of Utah, Salt Lake City, 1971.
- Perla, R. I., Slab Avalanche Measurements, *Can. Geotech. J.*, 14(2), 206–213, 1976.
- Petersson, P. E., Crack growth and development of fracture zone in plain concrete and similar materials, *Rep. TVBM-1006*, Div. of Bldg. Mater., Lund Inst. of Technol., Lund, Sweden, 1981.
- Rice, J. R., Mathematical analysis in the mechanics of fracture, in *Fracture—An Advanced Treatise*, vol. 2, edited by H. Liebowitz, pp. 191–308, Academic, San Diego, Calif., 1968.
- Zi, G., and Z. P. Bažant, Eigenvalue method for computing size effect of cohesive cracks with residual stress, with application to kink bands in composites, *Int. J. Eng. Sci.*, in press, 2003.

Z. P. Bažant and G. Zi, Department of Civil Engineering, Northwestern University, 2145 Sheridan Road, Evanston, IL 60208, USA. (z-bazant@northwestern.edu; g-zi@northwestern.edu)

D. McClung, Department of Geography, University of British Columbia, 217-1984 West Mall, Vancouver, B.C., Canada V6T 1Z2. (mcclung@geog.ubc.ca)